

REVIEW

Mechanically gated OSCA/TMEM63 ion channels: From physiological function to structural basis

 Siqi Deng^{1,2} , Qinling Qiu^{1,2} , Shangyu Dang^{1,3} , and Zhiqiang Yan^{4,5} 

The OSCA/TMEM63 family constitutes the largest identified group of mechanically gated ion channels, having pivotal roles in cellular mechanotransduction. OSCAs are osmosensitive and mechanically gated ion channels in plants, while their animal homologs TMEM63s similarly respond to mechanical stimuli and osmotic stress, characterized by smaller conductance and higher mechanoactivation thresholds. Structural studies suggest a conserved “force-from-lipid” gating mechanism for the OSCA/TMEM63 family, in which membrane tension or lipid bilayer curvature directly induces conformational changes and ion conductance. This review summarizes the physiological and pathological roles of OSCA/TMEM63 proteins, highlighting potential molecular mechanisms for their roles in mechanotransduction. Based on the structural homology and functional properties in biological membranes, we proposed a mechanically gated ion channel superfamily comprising OSCA/TMEM63 and TMC proteins.

Introduction

Force is a fundamental physical factor influencing biological processes in organisms and cells. All known life forms can sense and respond to mechanical forces. Mechanically gated ion channels, as primary force sensors, are widely distributed in prokaryotes and eukaryotes, transducing mechanical forces into electrical signals (Árnadóttir and Chalfie, 2010; Douguet and Honoré, 2019; Jin et al., 2020; Kefauver et al., 2020). Intriguingly, each mechanically gated ion channel family employs diverse force-gating mechanisms (Kefauver et al., 2020). Two primary models describe the gating mechanisms of mechanically gated ion channels: the force-from-lipids model, where membrane tension directly gates the channel through lipid bilayer deformation, and the tethered model, where force applied to the cell gates the channel indirectly via a linked tether (Cox et al., 2019; Douguet and Honoré, 2019; Jin et al., 2020; Kefauver et al., 2020).

The first discovered mechanically gated ion channels were the prokaryotic channels, the mechanosensitive channel of large conductance, and the mechanosensitive channel of small conductance, whose homologs are also found in archaea and plants (Sukharev et al., 1993; Kloda and Martinac, 2002; Haswell and Meyerowitz, 2006; Cox et al., 2019). Within eukaryotes, several channel families exhibit mechanosensitivity. No mechanoreceptor potential C (NomP_C), a transient receptor potential channel, is a mechanically gated ion channel in *Drosophila melanogaster* (Yan et al., 2013; Zhang et al., 2015; Wang et al., 2021). NomP_C acts as the mechanotransduction channel for gentle

touch in *Drosophila*, highly expressed and functionally essential in class III sensory neurons (Yan et al., 2013). PIEZOs, first identified in mammals as touch receptors (Ranade et al., 2014; Woo et al., 2014), have emerged as widely distributed molecular sensors critical for translating mechanical forces into biological signals across species. In animals, PIEZO channels are now linked to diverse mechanosensitive processes, including proprioception, lung function, urination, and bone development (Ranade et al., 2014; Woo et al., 2014; Nonomura et al., 2016; Sun et al., 2019; Marshall et al., 2020). Despite the versatile physiological significance of PIEZOs, multiple critical mechanotransduction pathways in animals operate through PIEZO-independent mechanisms. Auditory mechanotransduction, for instance, relies on the mechanically gated ion channels TMC1/2 in cochlear hair cells, where nanometer-scale deflection of stereociliary tip-links gates ion influx (Kawashima et al., 2011; Pan et al., 2013; Pan et al., 2018; Wu et al., 2017; Jia et al., 2020; Deng and Yan, 2025; Fu et al., 2025). PIEZO2 mediates touch sensation (Ranade et al., 2014; Woo et al., 2014) but not mechanical pain, and other unidentified mechanically gated ion channels may drive noxious mechanosensation. The discovery of previously unknown mechanically gated ion channel families remains critical in advancing our understanding of cellular mechanotransduction.

Among the newly identified mechanically gated ion channels, the OSCA/TMEM63 family emerges as the largest class conserved from plants to mammals (Murthy et al., 2018), integrating with

¹Division of Life Science, The Hong Kong University of Science and Technology, Hong Kong, China; ²Institute of Molecular Physiology, Shenzhen Bay Laboratory, Shenzhen, China; ³HKUST-Shenzhen Research Institute, Nanshan, China; ⁴Department of Neurobiology, School of Basic Medical Sciences, Capital Medical University, Beijing, China; ⁵Chinese Institute for Medical Physiology, Chinese Institutes for Medical Research, Beijing, China.

Correspondence to Zhiqiang Yan: zqyan@cimrbj.ac.cn; Shangyu Dang: sdang@ust.hk.

© 2026 Deng et al. This article is distributed under the terms as described at <https://rupress.org/pages/terms102024/>.

TMC families into a superfamily characterized by their similar architectures and functions. This review focuses on how OSCA/TMEM63 proteins bridge mechanotransduction to physiology and pathology, further highlighting unresolved questions in their gating mechanisms and therapeutic potential.

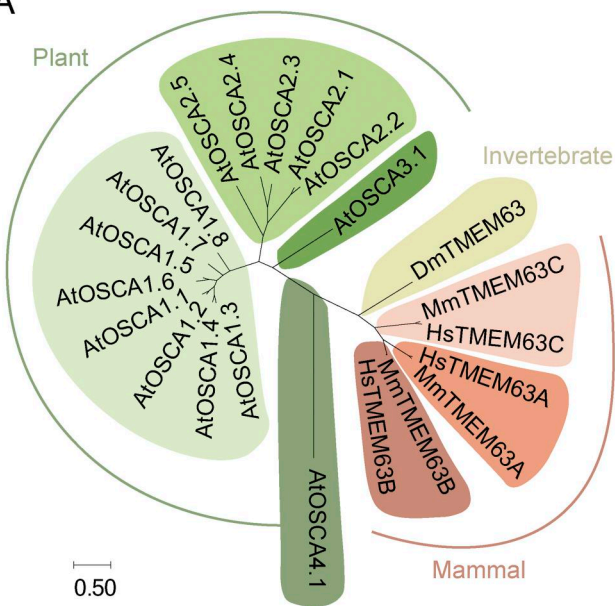
The OSCA/TMEM63 protein family as mechanically gated ion channels

The functions of OSCA family were first recognized in *Arabidopsis thaliana* in 2014, when OSCA1.1 was revealed as a hyperosmosensitive ion channel in guard cells (Hou et al., 2014; Yuan et al., 2014). In 2018, the OSCA family was identified as a new class of mechanically gated ion channels with the publication of their structures (Jojoa-Cruz et al., 2018; Murthy et al., 2018; Zhang et al., 2018), advancing the molecular understanding of mechanotransduction and initiating investigations into the versatile physiological functions of the OSCA/TMEM63 protein family. The evolutionary trajectory of the OSCA/TMEM63 family reveals remarkable functional conservation in mechanosensitivity, responding to mechanical stimuli with different activation thresholds (Murthy et al., 2018). OSCA/TMEM63 family proteins permeate biological kingdoms, positioning them at the frontier of cellular mechanotransduction: from 15 *A. thaliana* OSCA members (systematically named with numerical suffix, such as OSCA1.1) that gate stomatal closure during drought stress to three mammalian TMEM63 paralogs (TMEM63A, TMEM63B, and TMEM63C) that regulate sensory transduction and systemic homeostasis through mechanotransduction or osmotransduction pathways (Hou et al., 2014; Yuan et al., 2014; Murthy et al., 2018) (Fig. 1 A, Fig. 2 A, and Table 1). Heterologously expressed OSCA1.1 and OSCA1.2 can be activated by indenting the cell membrane with a glass probe under whole-cell patch clamp, demonstrating macroscopic mechanosensitive currents, or by applying negative pressure to the recording pipette to stretch the membrane in cell-attached or excised patch-clamp configurations (Murthy et al., 2018; Zhang et al., 2018). OSCA channels exhibit variations in unitary conductance and mechanical activation thresholds under negative pressure. OSCA1.1 and OSCA1.2 display large unitary conductances exceeding 100 pS, whereas OSCA3.1 has a higher activation threshold coupled with a lower conductance of less than 30 pS (Zhang et al., 2018; Han et al., 2024). In contrast to their plant orthologs, *Drosophila* TMEM63 and mammalian TMEM63A and TMEM63B only respond to higher stretch stimulation, with slower activation kinetics and unresolvable single-channel conductance (Li et al., 2021; Zhang et al., 2023a; Zheng et al., 2023; Chen et al., 2024; Li et al., 2024). In addition to mechanosensitivity, both TMEM63A and TMEM63B exhibit hypoosmosensitivity, while TMEM63B also retains conserved hyperosmosensitivity as OSCAs, possibly mediated by membrane curvature generated from osmolarity changes (Maity et al., 2019; Du et al., 2020; Zou et al., 2025). TMEM63C-expressing cells were found to respond to hyperosmolarity (Hou et al., 2014) and hypoosmolality (Du et al., 2020; Qin et al., 2023), but not to mechanical stimulation (Murthy et al., 2018). Beyond their gating by osmotic or mechanical stimuli, another

fundamental characteristic of OSCA/TMEM63 channels is their function as nonselective cation channels, a conserved characteristic observed from the initial discovery in AtOSCA1.1 to invertebrate and mammalian TMEM63s (Yuan et al., 2014; Murthy et al., 2018; Maity et al., 2019; Du et al., 2020; Li et al., 2024). Both plant and mammal subfamilies facilitate the permeation of monovalent (Na^+ and K^+) and divalent cations (Mg^{2+} , Ba^{2+} , and Ca^{2+}) (Yuan et al., 2014; Du et al., 2020), although the reports for their relative permeabilities of these cations are limited and vary between studies. Several key studies have reported significant Ca^{2+} permeability of OSCAs, mediating a direct role in calcium-mediated physiological processes in plants (Yuan et al., 2014; Thor et al., 2020; Pei et al., 2024), while other studies in mammalian TMEM63 have observed less Ca^{2+} conductance relative to monovalent cations (Du et al., 2020; Chen et al., 2024).

Structural analyses reflect lineage-specific oligomerizations of the OSCA/TMEM63 family. Plant OSCAs have homodimeric architecture with each protomer containing 11 transmembrane helices (TM0-TM10), of which TM3-TM7 function as the putative pore-forming helices (Jojoa-Cruz et al., 2018; Jojoa-Cruz et al., 2024a; Jojoa-Cruz et al., 2024b; Liu et al., 2018; Zhang et al., 2018; Maity et al., 2019; Han et al., 2024; Shan et al., 2024). The residues in the cytoplasmic domain between TM2 and TM3 (intracellular linker 2, IL2), along with some C-terminal residues form the dimer interface of OSCA proteins (Fig. 1 B). For example, in OSCA1.1, the dimer interface is stabilized by an extensive network of side chain and main chain interactions formed by IL2 residues Q339-R344 and C-terminal residues L686-E688 from both subunits (Zhang et al., 2018). In contrast, all high-resolution structures of TMEM63s reported so far suggest that the monomers are a dominant form (Qin et al., 2023; Zhang et al., 2023a; Zheng et al., 2023; Han et al., 2024; Miyata et al., 2024; Zheng et al., 2025), despite a small fraction of dimeric TMEM63B being observed using structural and biochemical approaches (Qin et al., 2023; Niu et al., 2024). Mammalian TMEM63A and TMEM63B, first resolved in closed states at 3.2 and 3.5 Å, respectively (Zhang et al., 2023a; Zheng et al., 2023), revealed two structural features that possibly contribute to their divergent oligomerization. First, in TMEM63A, TM10 rotates into the “central cavity,” and therefore sterically hinders the corresponding dimeric interface in its plant ortholog OSCAs (Zhang et al., 2023a). Second, the presence of additional amino acid residues in the IL2 domain of TMEM63B causes its corresponding β-hairpin loop to protrude horizontally, an alteration that likely interferes with dimer formation (Miyata et al., 2024). The cryo-EM structure of mouse TMEM63C, resolved at 3.56 Å resolution, was in monomeric configurations as its mammalian orthologs (Qin et al., 2023). This is further evidenced by the *in vivo* oligomerization analysis in the native state (Qin et al., 2023; Zheng et al., 2023). In TMEM63C, TM0, a membrane-contacting transmembrane helix, shifts toward TM6, displacing the cytoplasmic half of TM6 (named as TM6b) from its typical position in other TMEM63s near TM0 to a midpoint between TM0 and TM4 (Qin et al., 2023). Mutagenesis, together with cross-linking, confirms that TM0-TM6 coupling is essential for gating the ion transport pathway in TMEM63C (Qin et al., 2023).

A



B

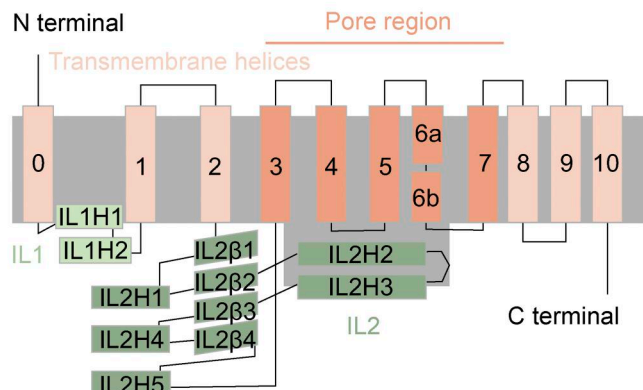


Figure 1. The evolutionarily conserved mechanically gated ion channels of OSCA/TMEM63 protein family. **(A)** Phylogenetic tree of OSCA/TMEM63 proteins across model plants *A. thaliana*, invertebrate *D. melanogaster*, mammal *Mus musculus*, and human *Homo sapiens*. For plant orthologs, OSCA are systematically named as OSCA1.1–8, OSCA2.1–5, OSCA3.1, and OSCA4.1, of which the numerical prefix indicates different subfamilies. There is only one copy of TMEM63 in *Drosophila*. Mammal orthologs, for both mouse and human, include three members of TMEM63A, TMEM63B, and TMEM63C. Sequences were aligned in Mega11 by maximum likelihood method. **(B)** Topology diagram of OSCA/TMEM63 with major transmembrane helices and structural components highlighted. The residues in cytoplasmic domain between TM0 and TM1 are named as IL1; those between TM2 and TM3 are named as IL2. Suffix "H" indicates a helix and "B" indicates a β sheet.

Electrophysiological studies revealed the functions of OSCA/TMEM63 in transducing mechanical stimuli (Murthy et al., 2018; Zhang et al., 2018; Zhang et al., 2023a; Zheng et al., 2023; Chen et al., 2024; Han et al., 2024; Li et al., 2024; Shan et al., 2024), while structural analyses uncover a fundamental divergence in their oligomeric states (Table 2). Given the evolutionarily conserved roles of the OSCA/TMEM63 family in mechanotransduction and osmotransduction, intensive researches have probed into the physiological relevance and the structural basis of their functions.

Physiological and pathological relevance of TMEM63 family

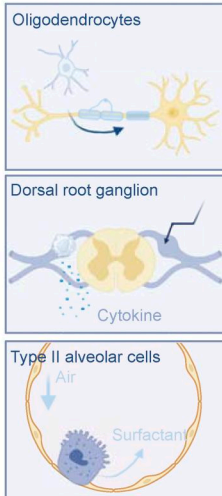
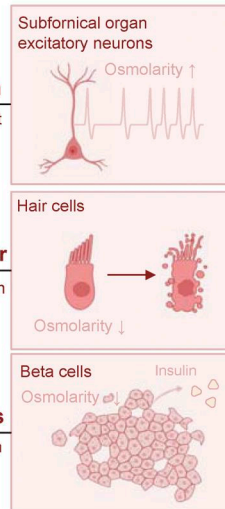
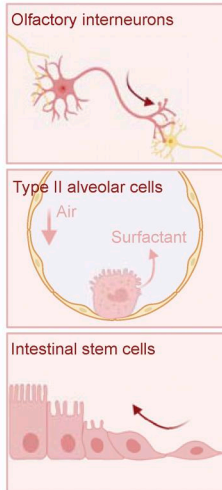
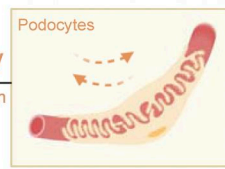
Studies in the past decade revealed the evolutionary conservation of OSCA/TMEM63 family proteins across plants and animals, underscoring their fundamental roles in cellular mechanotransduction. In plants, OSCAs are not only established to mediate drought tolerance and root hydrotropism but also function in fertilization (Yuan et al., 2014; Pei et al., 2024). Homologous to plant OSCAs, animal TMEM63 ion channels show significant functional diversification as mechanosensors, specializing in sensory transduction and systemic homeostasis; furthermore, some TMEM63 orthologs exhibit osmosensitivity akin to OSCAs, contributing to osmolarity-related physiological regulation (Fig. 2 A and Table 1).

TMEM63A governs diverse physiological processes across distinct tissues and cellular contexts, transducing the mechanical stimulation. TMEM63A is essential for normal myelination,

as evidenced by impaired myelination resulting from loss-of-function mutations in both mouse models and human patients (Yan et al., 2019; Tonduti et al., 2021; Fukumura et al., 2022; Halford et al., 2025). Highly enriched in oligodendrocytes (Fig. 2 B), TMEM63A may respond to mechanical force generated during myelin sheath formation through lipid biosynthesis and membrane expansion (Halford et al., 2025) (Fig. 2 A). Beyond regulating myelination, TMEM63A acts as a lysosomal mechanosensor essential for regulating the morphology and intracellular distribution of lysosomes (Li et al., 2024). The human TMEM63A residue G567, located on the pore-lining helix TM6 and linked to transient hypomyelination during infancy (Yan et al., 2019), is conserved in its *Drosophila* ortholog DmTMEM63, positioned at G540 correspondingly (Li et al., 2024). Flies with *Tmem63* knockout or the pathogenic G540S mutation exhibit impaired lysosomal degradation, synaptic loss, progressive motor deficits, and early death, recapitulating the symptoms of human TMEM63A-related diseases (Li et al., 2024).

TMEM63B serves as both a mechanosensor and an osmosensor. As a mechanosensor, TMEM63B (together with TMEM63A) couples mechanical forces from lung inflation to pulmonary surfactant secretion in the lamellar bodies of alveolar epithelial cells (Chen et al., 2024) (Fig. 2 A). As an osmosensor, the physiological relevance of the hypoosmosensitivity of TMEM63B was first identified in cochlear outer hair cells (Du et al., 2020) (Fig. 2 A). TMEM63B mediates Ca^{2+} -dependent regulatory volume decrease, a fundamental mechanism required for hair cell survival and auditory functions (Du et al., 2020). In addition to its hypoosmosensitivity, TMEM63B is established as a predominant hyperosmosensor

A

Mechanotransduction**TMEM63A****Osmotransduction****TMEM63B****TMEM63B****TMEM63C**

B

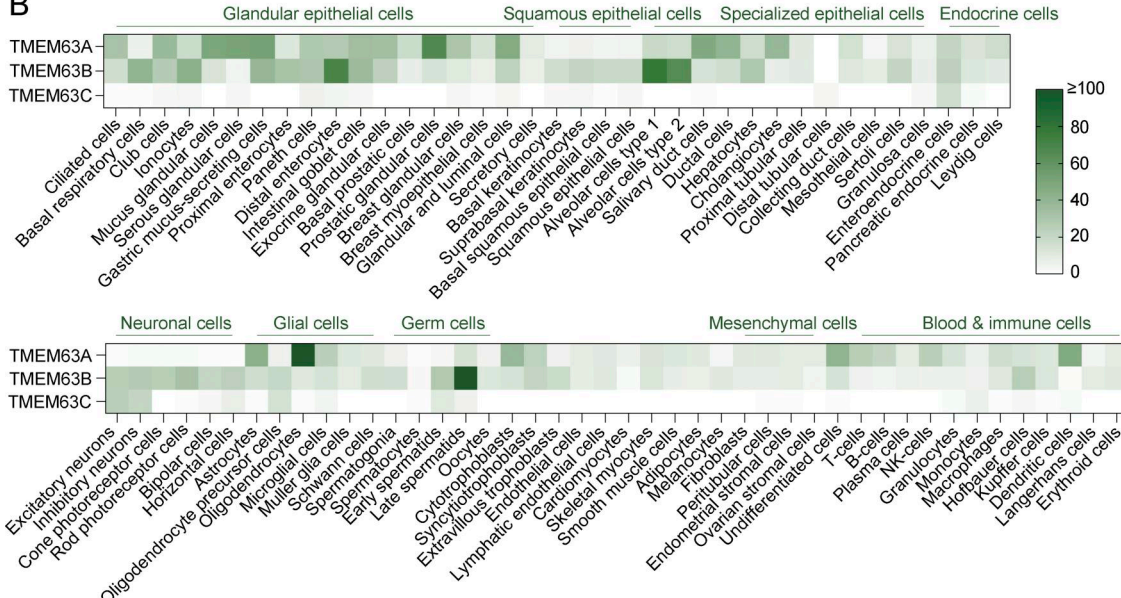


Figure 2. Expression and physiological functions of TMEM63s across human cell types. (A) Recent studies (referring to Table 1) reported the physiological and pathological roles of TMEM63A, TMEM63B, and TMEM63C in tissue-specific cell types, revealing their functions as mechanosensors and osmosensors. **(B)** Normalized transcript per million (nTPM) of TMEM63A, TMEM63B, and TMEM63C from Human Protein Atlas (HPA) database are displayed by heat map.

Table 1. Physiological roles of TMEM63 protein family

| Member | Expression | Related physiology/pathology | Ref |
|---------|--|---|--------------------------|
| TMEM63A | Oligodendrocytes and central nervous system | Mutations cause infantile hypomyelinating leukodystrophy | Yan et al. (2019) |
| | | Mutation identified in infantile hypomyelinating leukodystrophy | Tonduti et al. (2021) |
| | | Mutations cause infantile hypomyelinating leukodystrophy with global developmental delay | Fukumura et al. (2022) |
| | | Modulates myelin and myelin-associated protein production | Halford et al. (2025) |
| | Triple-negative breast cancer | Acts as an oncogene; involved in autophagy-mediated degradation pathway | Zhang et al. (2023b) |
| | Diffuse large B cell lymphoma | Potential therapeutic target; knockout inhibits diffuse large B cell lymphoma proliferation | Wu et al. (2022) |
| | Dorsal root ganglion neurons | Mediates macrophage infiltration and pro-inflammatory cytokine release, leading to pain hypersensitivity in chronic postamputation pain | Pu et al. (2023) |
| | Alveolar type 2 epithelial cells, lung | Mediates lung inflation-induced surfactant and ATP release | Chen et al. (2024) |
| | Alveolar type 2 epithelial cells, lung | Mediates lung inflation-induced surfactant and ATP release | Chen et al. (2024) |
| | | Regulates intestinal stem cell proliferation and motility | Tu et al. (2024) |
| TMEM63B | Subfornical organ neurons | Directly responds to hyperosmolarity in thirst | Zou et al. (2025) |
| | | Osmosensor detecting systemic hyperosmolarity for thirst drive | Yang et al. (2024) |
| | Cochlear sensory epithelial cells, inner ear | Regulates the regression of the greater epithelial ridge for normal onset of hearing | Ye et al. (2024) |
| | Outer hair cells and inner ear | Osmosensing regulates cell volume | Du et al. (2020) |
| | Brain | Gain-of-function variants cause neurodevelopmental disorder with epilepsy and neurodegeneration | Vetro et al. (2023) |
| | Pancreatic β -cells | Responds to glucose-induced swelling, triggering depolarization and insulin secretion | Tu et al. (2025) |
| | Olfactory interneurons | Mediates mechanical signaling for somal translocation during neuronal migration | Minegishi et al. (2025) |
| | Podocytes and kidney | Downregulated in angiotensin II-induced podocyte apoptosis | Eisenreich et al. (2020) |
| | | Downregulation causes podocyte loss; restoring TMEM63B rescues their viability | Orphal et al. (2020) |
| | | Essential for normal kidney filtration barrier function | Schulz et al. (2019) |
| TMEM63C | Nervous system | Dysfunction disrupts ER-mitochondrial contact sites in hereditary spastic paraparesis | Tábara et al. (2022) |

Summary of all established physiological and pathological functions of TMEM63s, including mechanosensation and osmoregulation processes in specific cell types.

(Zou et al., 2025) for thirst-driving water intake behavior in mouse models (Yang et al., 2024; Zou et al., 2025) (Fig. 2 A). As a molecular basis for osmotic thirst, TMEM63B is selectively enriched in subfornical organ excitatory neurons and necessary for their neuronal activation responding to hypertonic stimuli (Yang et al., 2024; Zou et al., 2025). The evolutionarily conserved function of TMEM63s in water homeostasis is demonstrated through the *Drosophila* TMEM63 ortholog in humidity-sensing and water-seeking behavior, with human TMEM63B successfully rescuing mutant phenotypes in cross-species complementation assays in flies (Li et al., 2022). The ubiquitous expression of TMEM63B across diverse cell types highlights its broad and essential roles in specialized physiology, necessitating further investigation (Fig. 2 B). Notably, *Tmem63b* isoforms, with an A-to-I RNA editing at exon 20 or an alternative splicing of exon 4, exhibit tissue-specific and age-related expression pattern, suggesting their distinct

physiological roles in different organs (Wu et al., 2020). The isoform lacking exon 4 constitutes ~80% of *Tmem63b* mRNA in the mouse brain but is undetectable in other tissues, indicating brain-specific alternative splicing (Wu et al., 2020). This short isoform of TMEM63B exhibits an enhanced response to hypoosmotic stimulation compared with the long isoform containing exon 4, possibly due to higher expression levels at the plasma membrane (Wu et al., 2020; Wu et al., 2023).

In contrast to its paralogs, the *in vivo* expression level of TMEM63C is relatively low and primarily localized to neurons (Fig. 2 B), where it possibly functions as an osmosensor in physiological conditions (Hou et al., 2014; Du et al., 2020; Qin et al., 2023). Investigations employing rat and zebrafish models, complemented by human genotype-phenotype correlation studies, have revealed TMEM63C functions in the critical selective interface of the kidney (Schulz et al., 2019) (Fig. 2 A). The osmosensitivity of TMEM63C (Hou et al., 2014; Du et al.,

Table 2. Structural elucidation of the OSCA/TMEM63 protein family summary of high-resolution structures of OSCA/TMEM63 channels, revealing their oligomeric states, pore architecture, lipid interactions, and functional states with mechanistic hints

| Protein | Species | PDB | Å | Detergent | Oligomerization | Functional state | Ref |
|---------------------------|---------------------|------|------|---------------------|-----------------|---|---------------------------|
| OSCA1.1 | <i>A. thaliana</i> | 6JPF | 3.52 | MNG, CHS | Dimer | Closed state | Zhang et al. (2018) |
| OSCA1.1 | <i>A. thaliana</i> | 8GRN | 2.5 | LMNG, CHS | Dimer | Closed state in nanodiscs | Zhang et al. (2023a) |
| OSCA1.1-F516A | <i>A. thaliana</i> | 8YMO | 2.7 | LMNG, CHS | Dimer | Pre-open state 1 | Shan et al. (2024) |
| OSCA1.1-F516A | <i>A. thaliana</i> | 8YMN | 2.5 | LMNG, CHS | Dimer | Pre-open state 2 | Shan et al. (2024) |
| OSCA1.1-F516A | <i>A. thaliana</i> | 8YMM | 2.8 | LMNG, CHS | Dimer | Open state | Shan et al. (2024) |
| OSCA1.1-F516A | <i>A. thaliana</i> | 8YMQ | 2.6 | LMNG, CHS | Dimer | Closed state in nanodiscs | Shan et al. (2024) |
| OSCA1.1-F516A | <i>A. thaliana</i> | 8YMP | 2.6 | LMNG, CHS | Dimer | Nanodisc in LPC | Shan et al. (2024) |
| OSCA1.2 | <i>A. thaliana</i> | 6MGV | 3.1 | LMNG, CHS | Dimer | Closed state in nanodiscs | Jojoa-Cruz et al. (2018) |
| OSCA1.2 | <i>A. thaliana</i> | 6MGW | 3.5 | LMNG, CHS | Dimer | Closed state | Jojoa-Cruz et al. (2018) |
| OSCA1.2 | <i>A. thaliana</i> | 6IJZ | 3.68 | GDN | Dimer | Closed state | Liu et al. (2018) |
| OSCA1.2 | <i>Oryza sativa</i> | 6OCE | 4.9 | DDM, sodium cholate | Dimer | Closed state | Maity et al. (2019) |
| OSCA1.2 | <i>A. thaliana</i> | 8T56 | 2.8 | DDM, CHS | Dimer | Closed state in Peptidiscs | Jojoa-Cruz et al. (2024a) |
| OSCA1.2 | <i>A. thaliana</i> | 8XS4 | 3.23 | DDM, CHS | Dimer | Contracted state 1: MSP:DOPC = 1:20 in nanodisc | Han et al. (2024) |
| OSCA1.2 | <i>A. thaliana</i> | 8XS5 | 3.33 | DDM, CHS | Dimer | Contracted state 2: MSP:DOPC = 1:20 in nanodisc | Han et al. (2024) |
| OSCA1.2 | <i>A. thaliana</i> | 8XNG | 3.56 | DDM, CHS | Dimer | Closed state: Liposome-inside-out | Han et al. (2024) |
| OSCA1.2 | <i>A. thaliana</i> | 8XAJ | 3.29 | DDM, CHS | Dimer | Open state:liposome-inside-in | Han et al. (2024) |
| OSCA1.2 | <i>A. thaliana</i> | 8XW2 | 3.59 | DDM, CHS | Dimer | Contracted state: MSP:DOPC = 1:50 in nanodisc | Han et al. (2024) |
| OSCA1.2 | <i>A. thaliana</i> | 8XW3 | 3.63 | DDM, CHS | Dimer | Expanded state: MSP:DOPC = 1:50 in nanodisc | Han et al. (2024) |
| OSCA1.2-V335W | <i>A. thaliana</i> | 8XW1 | 4.49 | DDM, CHS | Monomer | Closed state | Han et al. (2024) |
| OSCA2.3 | <i>A. thaliana</i> | 8T57 | 2.7 | DDM, CHS | Dimer | Closed state in Peptidiscs | Jojoa-Cruz et al. (2024a) |
| OSCA3.1 | <i>A. thaliana</i> | 5Z1F | 4.8 | MNG, CHS | Dimer | Closed state | Zhang et al. (2018) |
| OSCA3.1 | <i>A. thaliana</i> | 8GS0 | 3.3 | LMNG, CHS | Dimer | Expanded state | Zhang et al. (2023a) |
| OSCA3.1 | <i>A. thaliana</i> | 8GRO | 3.5 | LMNG, CHS | Dimer | Contracted state | Zhang et al. (2023a) |
| OSCA3.1 | <i>A. thaliana</i> | 8U53 | 2.6 | LMNG, CHS | Dimer | Closed state in nanodiscs | Jojoa-Cruz et al. (2024b) |
| OSCA3.1 | <i>A. thaliana</i> | 8XW0 | 3.11 | GDN | Dimer | Closed state | Han et al. (2024) |
| OSCA3.1-Y367N-G454S-Y458I | <i>A. thaliana</i> | 8XRY | 3.84 | GDN | Dimer | Open/open state | Han et al. (2024) |
| OSCA3.1-Y367N-G454S-Y458I | <i>A. thaliana</i> | 8XS0 | 3.89 | GDN | Dimer | Open/desensitized state | Han et al. (2024) |
| OSCA3.1-R611E-R619E | <i>A. thaliana</i> | 8XVY | 3.71 | GDN | Dimer | Closed/open state | Han et al. (2024) |
| OSCA3.1-R611E-R619E | <i>A. thaliana</i> | 8XVZ | 3.78 | GDN | Dimer | Closed/desensitized state | Han et al. (2024) |
| TMEM63A | <i>Homo sapiens</i> | 8GRS | 3.3 | LMNG, CHS | Monomer | Closed state | Zhang et al. (2023a) |
| TMEM63A | <i>Homo sapiens</i> | 8EHW | 3.8 | LMNG, CHS | Monomer | Closed state in nanodiscs | Zheng et al. (2023) |

Table 2. Structural elucidation of the OSCA/TMEM63 protein family summary of high-resolution structures of OSCA/TMEM63 channels, revealing their oligomeric states, pore architecture, lipid interactions, and functional states with mechanistic hints (Continued)

| Protein | Species | PDB | Å | Detergent | Oligomerization | Functional state | Ref |
|--------------|---------------------|------|------|-----------|-----------------|---------------------------------|--------------------------------------|
| TMEM63A | <i>Homo sapiens</i> | 8WUA | 3.6 | DDM, CHS | Monomer | Closed state | Wu et al. (2024) |
| TMEM63A-V53M | <i>Homo sapiens</i> | 9N95 | 3.65 | LMNG, CHS | Monomer | Closed state | Zheng et al. (2025) |
| TMEM63A-V53M | <i>Homo sapiens</i> | 9N93 | 2.95 | LMNG, CHS | Monomer | Lipid open state | Zheng et al. (2025) |
| TMEM63B | <i>Homo sapiens</i> | 8EHX | 3.6 | LMNG, CHS | Monomer | Closed state | Zheng et al. (2023) |
| TMEM63B | <i>Homo sapiens</i> | 8XW4 | 3.84 | GDN | Monomer | Closed state | Han et al. (2024) |
| TMEM63B | <i>Mus musculus</i> | 8WG3 | 3.4 | LMNG, CHS | Monomer | Closed state | Miyata et al. (2024) |
| TMEM63B | <i>Mus musculus</i> | 8WG4 | 3.5 | DDM, CHS | Monomer | Lipid open state with YN9303-24 | Miyata et al. (2024) |
| TMEM63C | <i>Mus musculus</i> | 8K0B | 3.56 | LMNG, CHS | Monomer | Closed state | Qin et al. (2023) |

MNG, maltose neopentyl glycol; CHS, cholestryl hemisuccinate; LMNG, lauryl maltose neopentyl glycol; DDM, n-dodecyl- β -D-maltopyranoside; GDN, digitonin; DOPC, dioleoylphosphatidylcholine; MSP, membrane scaffold protein.

2020; [Qin et al., 2023](#)) may play essential roles in maintaining the integrity of the glomerular filtration barrier ([Schulz et al., 2019](#)). Clinical studies also identified autosomal recessive TMEM63C variants as causes for hereditary spastic paraparesis, revealing the role of TMEM63C in dysregulated mitochondrial-ER dynamics as a fundamental pathomechanism for motor neuron degeneration ([Tábara et al., 2022](#)). However, whether TMEM63C's capacity in osmosensing plays a role in this physiological process remains unclear.

Structural elucidation of the OSCA/TMEM63 family suggests a mechano-gated mechanism

Research in the past decade has provided tremendous insights into the structures of OSCA/TMEM63 proteins from a range of organisms, revealing their oligomeric states, pore architecture, lipid interactions, and functional states with mechanistic hints ([Table 2](#)). Contrasting with plant OSCAs, where homodimer cooperativity may enhance mechano-activation, the distinct oligomerization of animal TMEM63s as monomers potentially contributes to their high-threshold mechanosensitivity and slow activation kinetics. Breaking the dimer configuration of OSCA1.2, either by replacing the dimer interface with the corresponding region from TMEM63A or applying a V335W mutagenesis, resulted in monomeric OSCA1.2 mutants, which present smaller channel conductance, higher activation thresholds, and slower activation kinetics ([Zheng et al., 2023; Han et al., 2024](#)). Nevertheless, monomeric OSCA1.2 mutants still showed faster activation kinetics compared with TMEM63s, indicating other structural features may also contribute to the relatively slow activation of TMEM63s compared with OSCAs ([Han et al., 2024](#)).

The force-form-lipid mechanism was proposed to activate OSCA/TMEM63 ion channels, in which lipids mediate force transduction via membrane tension or bilayer curvature ([Kefauver et al., 2020; Zheng et al., 2023; Han et al., 2024; Jojoa-Cruz et al., 2024b; Shan et al., 2024](#)). This mechanism was supported by the evidence that purified OSCA/TMEM63 proteins reconstituted in liposomes exhibit mechanosensitive activity under negative pressure ([Murthy et al., 2018; Zheng et al., 2023; Han et al., 2024](#)). In many mechanically gated ion channels, amphipathic helices function dually as anchors and deformation sensors of lipid membranes ([Brohawn et al., 2014; Bavi et al., 2016](#)), while similar structural features are also identified in OSCA/TMEM63 channels. An amphipathic helix between TM0 and TM1 (intracellular linker 1, IL1) in OSCA channels may be involved in sensing membrane tension ([Jojoa-Cruz et al., 2018; Jojoa-Cruz et al., 2024b](#)). Mutating the key residues of IL1 domain in OSCA1.2 abolishes pore responses while leaving stretch responses intact ([Jojoa-Cruz et al., 2018; Jojoa-Cruz et al., 2024b](#)). Additionally, two long amphipathic helices in IL2 (IL2H2 and IL2H3, also named as beam-like domain), linked via a membrane-anchored loop, are conserved across species in both OSCAs and TMEM63s, orienting parallel to the membrane and close to the internal membrane surface ([Jojoa-Cruz et al., 2018; Jojoa-Cruz et al., 2024b; Maity et al., 2019; Zheng et al., 2023](#)). These flexible cytosolic domains possibly act as potent sensors for membrane tension: when the membrane is stretched or curved, IL2H2 and IL2H3 may be positioned to detect the resulting mechanical force and coordinate movements of the pore-lining transmembrane helices to promote gate opening. Molecular dynamics (MD) simulations and electrophysiology in OSCA1.1 suggest that the critical pore-lining TM6 rearranges and straightens upon mechanoactivation, facilitating pore

dilation (Zhang et al., 2018), while simulations in TMEM63B showed transient contact between the cytoplasmic segment of TM6b and IL2H2, implicating the IL2H2/3-TM6 interaction in OSCA/TMEM63 gating (Zheng et al., 2023). Despite the conservation, conformational variations are identified between TMEM63s and OSCAs in the relative position of the putative membrane tension-sensing domain IL2H2/3 and the gating transmembrane domain TM6 (Maity et al., 2019; Zheng et al., 2023). IL2H2 and TM6, forming physical contact in OSCA1.2, does not form an obvious interaction in all available structures of TMEM63s, possibly contributing to the different activation thresholds of OSCA/TMEM63s (Zheng et al., 2023) (Fig. 3 A).

In addition to the aforementioned intracellular domains, recent structural analysis suggests the involvement of the extracellular domain in mechano-activation of OSCA/TMEM63. The extracellular regions of TM3-5 showed outward bending resembling a flower blooming in the open-state structures of OSCA1.2 and OSCA1.1-F516A (Han et al., 2024; Shan et al., 2024). The extracellular regions TM3a-Loop34-TM4a (EL3/4) and TM5a-Loop56 (EL5/6) segments in TMEM63s exhibit a hydrophobic network at the gate region (Zheng et al., 2025) (Fig. 3 A). The membrane-facing surfaces of the extracellular side of TM3-5 in TMEM63s are highly hydrophobic, enabling close association with the lipid bilayer (Zheng et al., 2025). These extracellular domains of OSCA/TMEM63s likely sense the alteration in membrane thickness and regulate the opening of the ion permeation pore (Zheng et al., 2025).

In summary, structural studies revealed different conformations and oligomeric states in OSCA/TMEM63 family members, governing their functional differences in unitary conductance and activation threshold. Studies in the mechano-activation of OSCA/TMEM63 proteins indicated a conserved “force-from-lipid” mechanism, possibly sensing membrane tension or curvature via the intracellular amphipathic helices (IL1 and IL2H2/3) and the extracellular pore-opening domains (EL3/4 and EL5/6). These hypothesized mechano-gating models, that the amphipathic helices of cytosolic or extracellular domains function as membrane tension sensors and interact with the pore-lining helix in OSCA/TMEM63, require further experimental evidence.

Mechano-activation process of OSCA/TMEM63 family proteins mediated by protein-lipid interaction

Recent advances in the field obtained the open-state structures of OSCA/TMEM63 proteins with different strategies, revealing critical insights into their mechano-activation processes (Han et al., 2024; Shan et al., 2024). Applying a “lipid titration” strategy to simulate mechanical tension enabled the capture of conducting-state OSCA1.2 structures (Han et al., 2024). In the open-state configuration in liposomes, OSCA1.2 adopts a contracted conformation with two protomers moving closer to each other than those in the closed state, while the pore-lining helices are clearly expanded (Han et al., 2024). These expanded and contracted states of OSCAs may reflect the general principle of mechanically gated ion channels governed by the force-from-lipids model, that their cross-sectional area within the

membrane plane increases in response to membrane tension (Jojoa-Cruz et al., 2018; Han et al., 2024). This phenomena is also found in *Caenorhabditis elegans* TMC1 (CeTMC1), a superfamily member of OSCAs, whose resolved structures similarly exhibit both expanded and contracted homodimeric configurations (Jeong et al., 2022). Additionally, structural observation revealed that the two protomers of OSCA1.2 can open independently (Han et al., 2024), raising the possibility that asymmetric activation enhances sensitivity to localized membrane tension. This asymmetric activation of OSCAs may explain the subconducting state identified in the patch-clamp recordings (Murthy et al., 2018; Han et al., 2024), though direct functional evidence for this mechanism remains to be established. Moreover, the open conformation of OSCA was also obtained by introducing mutants located at the constricted site of the pore, specifically F516A in OSCA1.1, which bypassed the technical difficulty of providing high-threshold force to the proteins (Shan et al., 2024). Similar to the open conformation of OSCA1.2, open-state OSCA1.1-F516A revealed the contraction of each protomer towards the dimer interface, with subsequent extrusion of lipids in the dimer interface (Han et al., 2024; Shan et al., 2024) (Fig. 3 B).

The activated pore of OSCA1.2 features a lateral opening to the membrane constructed by phospholipid headgroups, forming a hybrid protein-lipid pathway (Han et al., 2024). This “lipid wall” of an ion-permeable pathway redefines ion channel architecture, integrating lipids as structural cofactors (Fig. 3 B). The identity of the lipid headgroup, along with the residues lining the pore, shapes the ion permeation and selectivity of OSCA1.2 (Han et al., 2024). Besides pore-lining lipids, lipid-like densities within the pore fenestration were extensively identified in the structural analysis or MD simulation of OSCA/TMEM63 proteins (Zhang et al., 2023a; Zheng et al., 2023; Han et al., 2024; Jojoa-Cruz et al., 2024b), which may occlude ion conduction. The displacement of lipids that plug near the ion-permeable pore or bind to the cleft within transmembrane helices influences the mechano-gating of OSCA/TMEM63 proteins (Zhang et al., 2023a; Han et al., 2024; Jojoa-Cruz et al., 2024b; Shan et al., 2024). For example, in the tension-insensitive OSCA3.1, a tightly bound “interlocking lipid” wedges into the central cleft (near TM3-TM4), stabilizing the closed conformation (Han et al., 2024). Mutating residues that coordinate lipids in OSCA3.1 triggers constitutive activation of channels without mechanical stimuli, demonstrating these lipids as gating “locks” (Han et al., 2024).

Despite the current understanding about the activation process of OSCA channels under mechanical stimulation, whether TMEM63 channels employ a similar mechanism remains speculative, given that their monomeric architecture implies divergent gating strategies. Resolving open-state structures of TMEM63s is imperative to elucidate how TM6 rearrangement, lipid interactions, and potential dimerization contribute to pore opening and ion permeability under mechanical stimulation. Further, considering that OSCA/TMEM63 family members diverge in the extent of mechanosensitivity and osmosensitivity, another critical question is how the molecular gating mechanism confers OSCA/TMEM63 family members with these diverse properties. Although osmotic stress alters membrane tension, the concurrent changes in ion concentration during osmotic

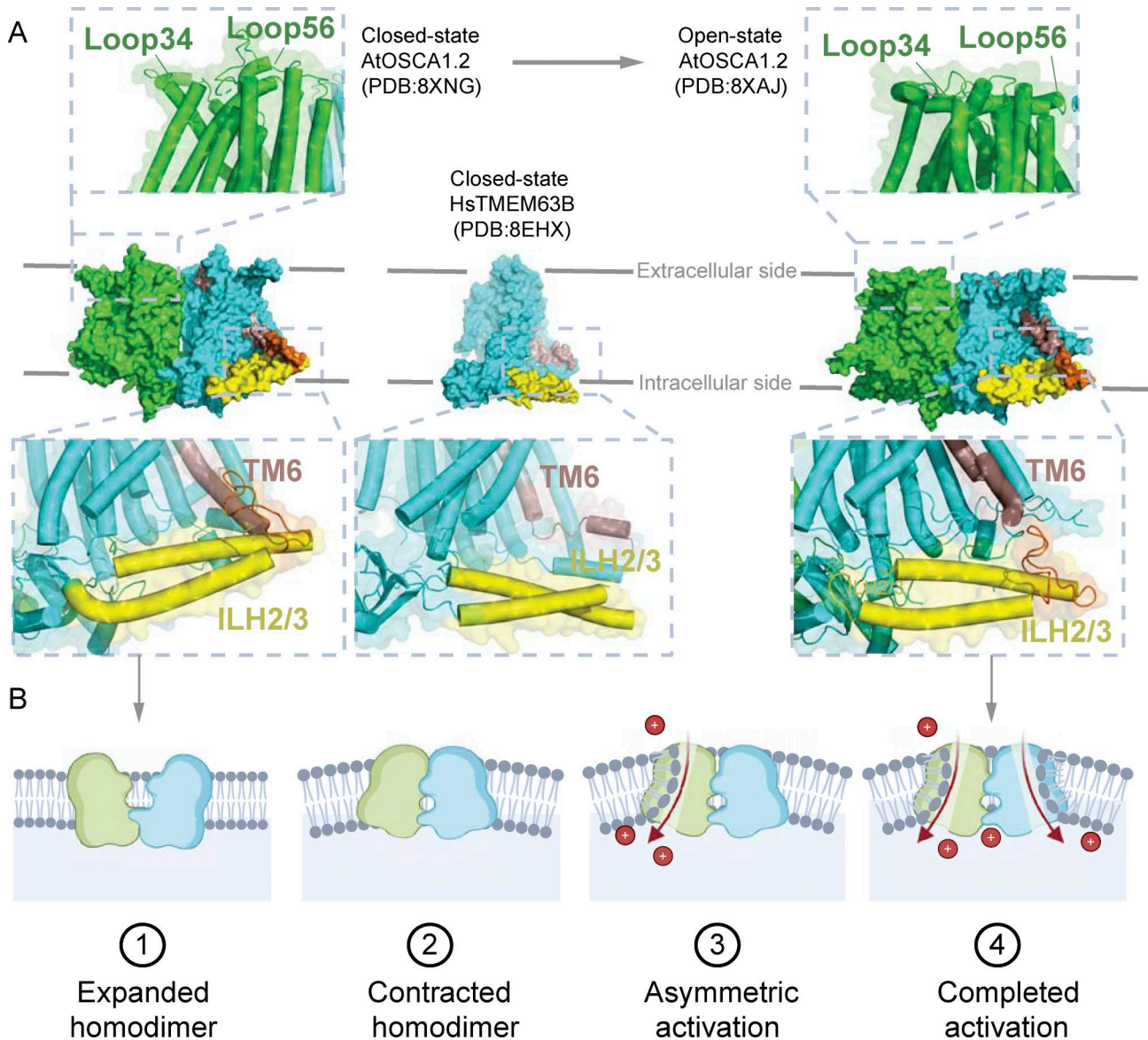


Figure 3. Proposed gating mechanism and activation process of OSCA/TMEM63 mechanically gated ion channels. Schematic depicting conformational transitions between closed and activated states of OSCA/TMEM63s during mechanical force transduction. **(A)** Extracellular domains of OSCA/TMEM63s, TM3a–Loop34–TM4a, and TM5a–Loop56, putatively sense the alteration in membrane thickness and stabilize the open conformation; intracellular amphipathic helices linked via a membrane-anchored loop, IL2H2 and IL2H3, possibly act as the sensors for membrane tension, coordinating movements of the transmembrane helix TM6. **(B)** Expanded and contracted homodimer conformations under closed and open states with asymmetric activation of protomers in OSCA channels. Open-state conformation of OSCA/TMEM63 proteins revealed a proteo-lipidic conducting pore.

Downloaded from <http://jcbpress.org/jcb/article-pdf/225/2/e202507014/202507014.pdf> by guest on 09 February 2026

perturbation make it mechanistically distinct from direct mechanical stimuli. Resolving this mechanistic foundation of the OSCA/TMEM63 family requires deeper investigation into the structural and dynamic bases of the tension-sensing specificity in their mechanosensitivity and osmosensitivity.

A superfamily of mechanically gated channels OSCA/TMEM63 and TMC proteins defined by shared structural homology

Unified by structural homology, the OSCA/TMEM63 and TMC families collectively form a mechanically gated ion channel superfamily, revealing a similar architecture among the

transmembrane domains and dimer assemblies that contain two pores with one in each protomer (except monomeric TMEM63s). The TMC protein family has attracted abundant attention since TMC1/2 are recognized as auditory mechanotransducer candidates (Kurima et al., 2002; Vreugde et al., 2002; Kawashima et al., 2011; Pan et al., 2013; Pan et al., 2018). Recent *in vitro* studies have overcome the long-standing challenge of localizing TMC1/2 to the cell membrane in heterologous systems, establishing their role as the pore-forming subunits of mechanically gated ion channels (Jia et al., 2020; Chen et al., 2025; Fu et al., 2025). The hearing loss phenotype in *Tmc1* mutant mice, the expression of TMC1/2 at auditory mechanotransduction sites and their inherent mechanosensitivity collectively provide

compelling evidence for TMC1/2 to meet both the essential and necessary criteria as the molecular mechanotransducer in hair cells for auditory function (Kawashima et al., 2011; Jia et al., 2020; Chen et al., 2025; Deng and Yan, 2025; Fu et al., 2025). In hair cells, mechanical force is transmitted to TMC1/2 channels via tip links. However, it remains unclear whether these channels are activated via a tether-based mechanism or via changes in local membrane tension (Gillespie and Müller, 2009; Zheng and Holt, 2021). Crucially, these two mechanisms are not mutually exclusive and may work in synergy (Deng and Yan, 2025). The establishment of TMC1/2 mechanosensitivity necessitates expanded investigation of TMC3–8 family members, whose diverse physiological roles require further elucidation of the underlying molecular mechanism (Kurima et al., 2003; Kortmann et al., 2023; Wang et al., 2024). OSCA/TMEM63 and TMC proteins are also architecturally related to TMEM16 proteins, sharing homologous dimer conformations that define them as the TOSCA superfamily (Jan and Jan, 2025), the transmembrane channel scramblase superfamily (Le et al., 2021; Mun and Holt, 2025), or the anoctamin superfamily (Medrano-Soto et al., 2018). While TMEM16A and TMEM16B function as Ca^{2+} -activated chloride channels (Caputo et al., 2008; Schroeder et al., 2008; Yang et al., 2008), several members of TMEM16 family (e.g., TMEM16D and TMEM16F) (Jan and Jan, 2025), OSCA/TMEM63 (Yuan et al., 2014; Murthy et al., 2018; Maity et al., 2019; Du et al., 2020; Li et al., 2024), and TMC proteins (Jia et al., 2020; Fu et al., 2025) are known as cation channels. In addition, studies revealing the lipid scramblase activity of TMEM16D, TMEM16E, TMEM16F, and TMEM16K established them as dual-function proteins (Le et al., 2021; Jan and Jan, 2025).

Shared structural features were identified between OSCA/TMEM63 and TMC families, indicating similar dynamic processes of TM6 in channel activation under mechanical stimulation. In the structurally related TMEM16A, the pore-lining TM6 directly binds calcium ions and undergoes significant conformational changes during ion permeation. This observation has led to the proposal that TM6 functions as a gating helix, coupling calcium sensing and pore opening in TMEM16A (Dang et al., 2017; Peters et al., 2018). Strikingly, TMEM16 scramblases utilize a hydrophilic groove between TM4 and TM6 to enable lipid headgroup translocation, anchoring hydrophobic tails in the membrane interior (Feng et al., 2019; Le et al., 2019; Arndt et al., 2022; Jan and Jan, 2025). Recent structural and functional studies on OSCA/TMEM63 and TMC proteins provide evidence that this proteo-lipidic composition possibly extends beyond TMEM16 family members, functioning as the ion-permeable pathway for mechanically gated ion channels. Structural analyses of OSCAs and TMEM63s reveal a similar π -helix on TM6 (Jojoa-Cruz et al., 2018; Zheng et al., 2023), a distinctive structural motif characterized by a wider diameter and more residues per turn compared with a standard π -helix. This unique architecture of π -helix on TM6 is thought to introduce inherent strain and flexibility, making it a potential molecular pivot that facilitates the rearrangement of TM6 for pore dilation. Intriguingly, the TM6 shifting observed in open-state OSCA/TMEM63 proteins leads to a lateral opening surrounded by both TM4 and

TM6, exposing to the lipid membrane (Han et al., 2024; Miyata et al., 2024; Zheng et al., 2025). Furthermore, the π -helix on TM6 is also present in *C. elegans* TMC1 and TMC2, possibly undergoing a π - to α -helix transition during activation (Clark et al., 2024). Notably, mutagenesis studies targeting the equivalent domain in mouse TMC1 demonstrated that TM4 and TM6 is critical for mechanotransduction currents in auditory hair cells, of which the corresponding mutations extensively cause human deafness in clinical cases (Pan et al., 2013; Pan et al., 2018; Akyuz et al., 2022). Structural studies and MD simulation have revealed shared features of lipid-lined pores in TMC1 and OSCAs for ion permeation with the lipidic wall locating between TM4 and TM6, indicating a potentially similar activation process (Walujkar et al., 2021, Preprint; Han et al., 2024).

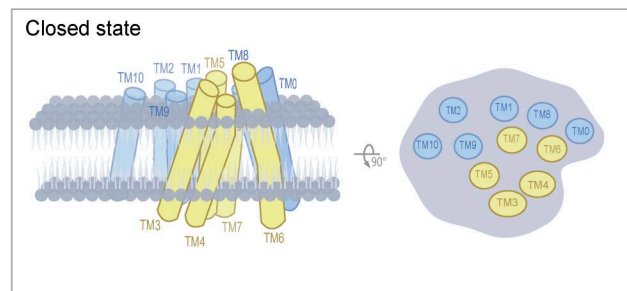
The molecular mechanism underlying the functions of these structurally similar proteins requires further elucidation. The relationship between the lipid translocation pathway and the ion-conducting pore in TMEM16 proteins presents a fundamental choice between two mechanisms: a single shared proteo-lipidic conduit for both ion conduction and lipid scrambling simultaneously, or distinct spatially segregated domains—potentially competing—performing these functions separately (Fig. 4). A shared hybrid proteo-lipidic ion conduction mechanism in OSCA/TMEM63s is evidenced by a membrane tension-gated lateral opening between TM4 and TM6 that permits lipid headgroups to infiltrate the pore, complemented by the direct influence of lipid composition on the channel's ion permeability (Han et al., 2024). For TMC proteins, MD simulation of TMC1 in lipid membrane suggests an intermediate state before the conducting state, where the pore widens with separation of TM4/6 and lipid headgroups block conductance; subsequently shifting TM4 and TM6 may laterally drag the pore lipid headgroups to line the ion permeable pathway instead of blocking it (Walujkar et al., 2021, Preprint). This dynamic analysis of TMC1 provides integrated models for both the shared proteo-lipidic conduit and the functional competition of lipid and ion influx. Moreover, the composition and biophysical influence of phospholipids and cholesterol within the pores of this structural superfamily also demand systematic analysis. Elucidation is required on how headgroup charge, acyl chain saturation, and sterol interactions modulate proteo-lipidic pore dynamics and gating behavior.

To summarize, structural biology analysis raises an emerging possibility that a similar “proteo-lipidic pore” existed in the mechanically gated ion channel superfamily of OSCA/TMEM63 and TMC. This speculative model is inspired by their shared reliance on the TM6 helix as an essential gating element, while still requiring further investigation in the dynamic mechanism for both ion conductance and lipid translocation.

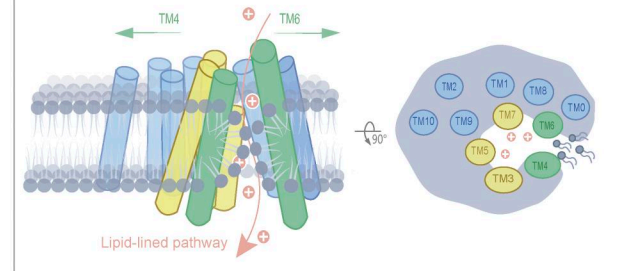
Conclusion and perspectives

The discovery of mechanically gated ion channels has revolutionized our understanding of cellular mechanotransduction, of which each protein family has diverse gating mechanisms to transduce mechanical stimulation into electrical signals. Although multiple eukaryotic ion channels have been previously described, limited members are conserved from plants to

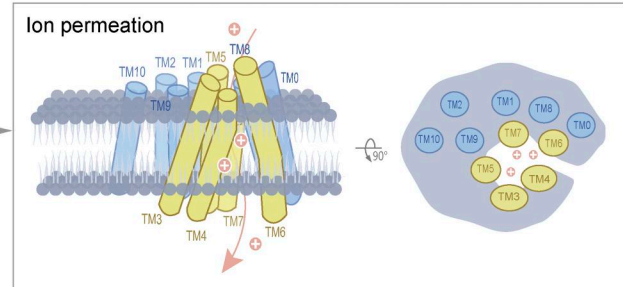
A Shared proteo-lipidic pathway



Ion permeation+lipid translocation



B Mutually exclusive ion permeation and lipid translocation



Lipid translocation

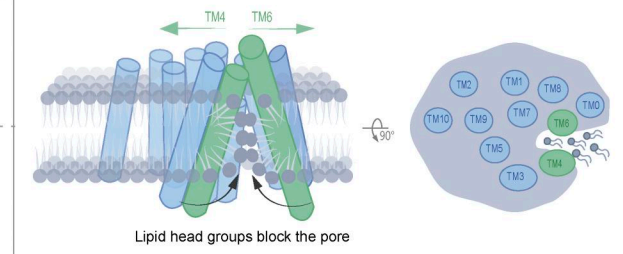


Figure 4. Proposed functional mechanisms of TMEM16, OSCA/TMEM63, and TMC super family. (A) A shared proteo-lipidic conduit mediating ion conduction lined with lipid headgroups. OSCA/TMEM63s under membrane tension or TMEM16s with Ca^{2+} binding may undergo conformational changes that dilate a central ion-permeable pore lined by lipid headgroups and conserved hydrophilic residues. (B) Spatially competition of ion permeation and lipid translocation. Ion permeation and lipid translocation may occur through physically distinct but allosterically coupled pathways in TMEM16s. TMC1 may employ a stepwise activation mechanism, such that subsequently shifting TM4 and TM6 may laterally drag the pore lipid headgroups to line the ion permeable pathway instead of blocking it.

humans. OSCA/TMEM63 and TMC proteins potentially represent the largest superfamily of mechanically gated ion channels among the eukaryotes known to date (Murthy et al., 2018). Future research targeting OSCA/TMEM63 family will center on two interconnected aspects essential to advancing the understanding of cellular mechanotransduction. First, the unexplored physiological functions of TMEM63s across tissue-specific contexts should be elucidated, where these mechanosensors mediate critical yet poorly understood pathophysiological processes. Concurrently, resolving the precise molecular gating mechanisms underpinning the force-from-lipid activation of OSCA/TMEM63 proteins remains imperative. These dual-axis researches in TMEM63 family will bridge mechanistic insights of mechanically gated ion channels with their emergent biological roles, ultimately illuminating therapeutic strategies for clinical disorders.

Animal TMEM63 proteins, functioning as both mechanosensors and osmosensors, have emerged with implications in neural development, auditory function, pulmonary homeostasis, and renal filtration, among other functions. Future research efforts must integrate tissue-specific expression mapping of TMEM63 isoforms and clinical reports with functional phenotypes to elucidate their unexplored physiological and pathological roles. The physiological relevance of TMEM63s reveal therapeutic potential of targeting these mechanosensors—from engineering mechanically gated channel activities to developing

lipid-corrective interventions. For example, regulating TMEM63A function may promote remyelination in multiple sclerosis or leukodystrophies, potentially via sensitizing the channel to mechanical stimulation during oligodendrocyte maturation (Yan et al., 2019; Fukumura et al., 2022; Chen et al., 2024). Targeting TMEM63B represents a conceptually promising strategy for epilepsy by stabilizing neuronal excitability, disorders of fluid balance, and diabetes insipidus (Vetro et al., 2023; Yang et al., 2024; Tu et al., 2025; Zou et al., 2025). Understanding TMEM63C's role in hereditary spastic paraparesis could reveal whether modulating its functions might provide neuroprotection in stressed axons (Tábara et al., 2022). However, these approaches remain hypothetical in the absence of selective pharmacological agents for any member of the TMEM63 family, a fundamental challenge that must be overcome in future work.

Having known the mechanosensitivity and osmosensitivity of OSCA/TMEM63 family, structural breakthroughs unveiled the dominant force-from-lipid gating paradigm of OSCA/TMEM63 family where membrane tension directly induces conformational changes through lipid–channel interactions, bypassing protein tethers used by other mechanically gated ion channels such as NompC (Zhang et al., 2015; Wang et al., 2021). Hypotheses have posited that extracellular domains of the pore-lining helices TM3–TM5 (EL3/4 and EL5/6) or intracellular amphipathic domains (IL1 and IL2H2/3) collectively sense membrane tension to drive pore opening. Nevertheless, these

proposed membrane-sensing domains have not been fully tested, and comprehensive molecular understanding demands rigorous validation through (1) obtaining high-resolution open-state structures of the mechanically gated ion channel TMEM63s, ideally in different lipid environments (Tao et al., 2023; Liu et al., 2025), to visualize the gating transition directly; (2) conducting a systematic electrophysiological dissection of putative lipid-interacting and force-transmitting residues; and (3) developing specific pharmacological or genetic tools to probe the functional contribution of each proposed sensor domain *in vivo*.

From a structural perspective, OSCA/TMEM63 and TMC proteins form a superfamily of mechanically gated channels featured by similar dimer configurations and a proteo-lipidic pore architecture. These shared structural features potentially imply similar gating principles of OSCA/TMEM63 and TMC proteins, opening avenues to explore how the core gating motifs (e.g., the TM6 π -helix) enable mechanotransduction across physiological contexts. Cross-family screening of compounds targeting these shared functional domains could further yield allosteric modulators for channelopathy therapeutics. Future studies should also explore the functional diversity of this structural superfamily, specifying if the members exclusively perform one function, either as an ion channel or lipid scramblase, or perform both roles. For example, systematically investigating whether TMEM16 proteins, primarily identified as calcium-activated channels or lipid scramblases, exhibit mechanosensitivity as the structurally related OSCA/TMEM63 proteins could uncover a new force-sensing mechanism. Furthermore, beyond mechanically gated ion channels, mutant OSCA/TMEM63s were recently identified as lipid scramblases, reminiscent of TMEM16s (Lowry et al., 2024; Zheng et al., 2025). Pathogenic mutations V44M and R433H lock TMEM63B in a hyperactive state, causing membrane blebbing and neurodevelopmental defects (Miyata et al., 2024; Niu et al., 2024). Resembling TMEM63B-V44M, TMEM63A with mutation V53M at the homologous sites was also found to induce constitutive lipid scramblase activity, while the channel activity of the mutant TMEM63A protein is not enhanced or equipped with leak current (Zheng et al., 2025). Notably, the obtained open structures of TMEM63B and mutant TMEM63A are characteristic of a lipid-open state—a configuration that enables lipid passage through the lateral opening between TM4 and TM6 (Miyata et al., 2024; Zheng et al., 2025). It is speculated that these may differ from a yet-to-be-determined, fully dilated ion-open state in TMEM63s (Zheng et al., 2025).

Acknowledgments

This work was supported by funds from the STI2030-Major Projects (2021ZD0203304), Shenzhen Medical Research Funding (B2302032), National Key R&D Program of China Project (2021YFA1101302), National Natural Science Foundation of China (31970931), National Natural Science Foundation of China (32525033), Shenzhen Science and Technology Program (RCJC20210609104631084) (to Z. Yan), Hong Kong Research Grants Council (GRF16102822, GRF16100223, C6001-21E, and

C6012-22G), HKUST VPRDO 30-for-30 Research Initiative Scheme, and HKUST start-up and initiation grants (to S. Deng). The authors apologize to colleagues whose important works are not cited here due to space limitations.

Author contributions: Siqi Deng: conceptualization, data curation, formal analysis, investigation, methodology, project administration, software, validation, visualization, and writing—original draft, review, and editing. Qinling Qiu: conceptualization, formal analysis, investigation, visualization, and writing—original draft, review, and editing. Shangyu Dang: conceptualization, funding acquisition, resources, supervision, and writing—review and editing. Zhiqiang Yan: conceptualization, data curation, formal analysis, funding acquisition, investigation, methodology, project administration, resources, software, supervision, validation, visualization, and writing—original draft, review, and editing.

Disclosures: The authors declare no competing interests exist.

Submitted: 30 July 2025

Revised: 11 November 2025

Accepted: 2 December 2025

References

Akyuz, N., K.D. Karavitaki, B. Pan, P.I. Tamvakologos, K.P. Brock, Y. Li, D.S. Marks, and D.P. Corey. 2022. Mechanical gating of the auditory transduction channel TMC1 involves the fourth and sixth transmembrane helices. *Sci. Adv.* 8:eab0126. <https://doi.org/10.1126/sciadv.ab0126>

Árnadóttir, J., and M. Chalfie. 2010. Eukaryotic mechanosensitive channels. *Annu. Rev. Biophys.* 39:111–137.

Arndt, M., C. Alvadía, M.S. Straub, V. Clerico Mosina, C. Paulino, and R. Dutzler. 2022. Structural basis for the activation of the lipid scramblase TMEM16F. *Nat. Commun.* 13:6692. <https://doi.org/10.1038/s41467-022-34497-x>

Bavi, N., D.M. Cortes, C.D. Cox, P.R. Rohde, W. Liu, J.W. Deitmer, O. Bavi, P. Strop, A.P. Hill, D. Rees, et al. 2016. The role of Mscl amphipathic N terminus indicates a blueprint for bilayer-mediated gating of mechanosensitive channels. *Nat. Commun.* 7:11984. <https://doi.org/10.1038/ncomms11984>

Brohawn, S.G., Z. Su, and R. MacKinnon. 2014. Mechanosensitivity is mediated directly by the lipid membrane in TRAAK and TREK1 K⁺ channels. *Proc. Natl. Acad. Sci. USA.* 111:3614–3619. <https://doi.org/10.1073/pnas.1320768111>

Caputo, A., E. Caci, L. Ferrera, N. Pedemonte, C. Barsanti, E. Sondo, U. Pfeffer, R. Ravazzolo, O. Zegarra-Moran, and L.J.V. Galietta. 2008. TMEM16A, a membrane protein associated with calcium-dependent chloride channel activity. *Science.* 322:590–594. <https://doi.org/10.1126/science.1163518>

Chen, G.-L., J.-Y. Li, X. Chen, J.-W. Liu, Q. Zhang, J.-Y. Liu, J. Wen, N. Wang, M. Lei, J.P. Wei, et al. 2024. Mechanosensitive channels TMEM63A and TMEM63B mediate lung inflation-induced surfactant secretion. *J. Clin. Invest.* 134:e174508. <https://doi.org/10.1172/JCI174508>

Chen, Y., Y. Li, Y. Liu, J. Sun, W. Feng, Y. Chen, Y. Tian, T. Lei, and P. Huang. 2025. Ectopic mouse TMC1 and TMC2 alone form mechanosensitive channels that are potently modulated by TMIE. *Proc. Natl. Acad. Sci. USA.* 122:e2403141122. <https://doi.org/10.1073/pnas.2403141122>

Clark, S., H. Jeong, R. Posert, A. Goehring, and E. Gouaux. 2024. The structure of the *Caenorhabditis elegans* TMC-2 complex suggests roles of lipid-mediated subunit contacts in mechanosensory transduction. *Proc. Natl. Acad. Sci. USA.* 121:e2314096121. <https://doi.org/10.1073/pnas.2314096121>

Cox, C.D., N. Bavi, and B. Martinac. 2019. Biophysical principles of ion-channel-mediated mechanosensory transduction. *Cell Rep.* 29:1–12. <https://doi.org/10.1016/j.celrep.2019.08.075>

Dang, S., S. Feng, J. Tien, C.J. Peters, D. Bulkley, M. Lolicato, J. Zhao, K. Zuberbühler, W. Ye, L. Qi, et al. 2017. Cryo-EM structures of the TMEM16A calcium-activated chloride channel. *Nature.* 552:426–429. <https://doi.org/10.1038/nature25024>

Deng, S., and Z. Yan. 2025. TMC1 and TMC2 function as the mechano-electrical transduction ion channel in hearing. *Curr. Opin. Neurobiol.* 93:103026. <https://doi.org/10.1016/j.conb.2025.103026>

Douguet, D., and E. Honoré. 2019. Mammalian mechano-electrical transduction: Structure and function of force-gated ion channels. *Cell.* 179: 340–354. <https://doi.org/10.1016/j.cell.2019.08.049>

Du, H., C. Ye, D. Wu, Y.-Y. Zang, L. Zhang, C. Chen, X.-Y. He, J.-J. Yang, P. Hu, Z. Xu, et al. 2020. The cation channel TMEM63B is an osmosensor required for hearing. *Cell Rep.* 31:107596. <https://doi.org/10.1016/j.celrep.2020.107596>

Eisenreich, A., M. Orphal, K. Böhme, and R. Kreutz. 2020. Tmem63c is a potential pro-survival factor in angiotensin II-treated human podocytes. *Life Sci.* 258:118175. <https://doi.org/10.1016/j.lfs.2020.118175>

Feng, S., S. Dang, T.W. Han, W. Ye, P. Jin, T. Cheng, J. Li, Y.N. Jan, L.Y. Jan, and Y. Cheng. 2019. Cryo-EM studies of TMEM16F calcium-activated ion channel suggest features important for lipid scrambling. *Cell Rep.* 28: 1385–1397. <https://doi.org/10.1016/j.celrep.2019.07.052>

Fu, S., X. Pan, M. Lu, J. Dong, and Z. Yan. 2025. Human TMC1 and TMC2 are mechanically gated ion channels. *Neuron.* 113:411–425.e4. <https://doi.org/10.1016/j.neuron.2024.11.009>

Fukumura, S., T. Hiraide, A. Yamamoto, K. Tsuchida, K. Aoto, M. Nakashima, and H. Saitsu. 2022. A novel de novo TMEM63A variant in a patient with severe hypomyelination and global developmental delay. *Brain Dev.* 44:178–183. <https://doi.org/10.1016/j.braindev.2021.09.006>

Gillespie, P.G., and U. Müller. 2009. Mechanotransduction by hair cells: Models, molecules, and mechanisms. *Cell.* 139:33–44. <https://doi.org/10.1016/j.cell.2009.09.010>

Halford, J., A.J. Senatore, S. Berryman, A. Muñoz, D. Semidey, R.A. Doan, A.M. Coombs, B. Noimany, K. Emberley, B. Emery, et al. 2025. TMEM63A, associated with hypomyelinating leukodystrophies, is an evolutionarily conserved regulator of myelination. *Proc. Natl. Acad. Sci. USA.* 122: e2507354122. <https://doi.org/10.1073/pnas.2507354122>

Han, Y., Z. Zhou, R. Jin, F. Dai, Y. Ge, X. Ju, X. Ma, S. He, L. Yuan, Y. Wang, et al. 2024. Mechanical activation opens a lipid-lined pore in OSCA ion channels. *Nature.* 628:910–918. <https://doi.org/10.1038/s41586-024-07256-9>

Haswell, E.S., and E.M. Meyerowitz. 2006. MscS-like proteins control plastid size and shape in *Arabidopsis thaliana*. *Curr. Biol.* 16:1–11. <https://doi.org/10.1016/j.cub.2005.11.044>

Hou, C., W. Tian, T. Kleist, K. He, V. Garcia, F. Bai, Y. Hao, S. Luan, and L. Li. 2014. DUF221 proteins are a family of osmosensitive calcium-permeable cation channels conserved across eukaryotes. *Cell Res.* 24:632–635. <https://doi.org/10.1038/cr.2014.14>

Jan, L.Y., and Y.N. Jan. 2025. Wide-ranging cellular functions of ion channels and lipid scramblases in the structurally related TMC, TMEM16 and TMEM63 families. *Nat. Struct. Mol. Biol.* 32:222–236. <https://doi.org/10.1038/s41594-024-01444-x>

Jeong, H., S. Clark, A. Goehring, S. Dehghani-Ghahnaviyeh, A. Rasouli, E. Tajkhorshid, and E. Gouaux. 2022. Structures of the TMC-1 complex illuminate mechanosensory transduction. *Nature.* 610:796–803. <https://doi.org/10.1038/s41586-022-05314-8>

Jia, Y., Y. Zhao, T. Kusakizako, Y. Wang, C. Pan, Y. Zhang, O. Nureki, M. Hattori, and Z. Yan. 2020. TMC1 and TMC2 proteins are pore-forming subunits of mechanosensitive ion channels. *Neuron.* 105:310–321.e3. <https://doi.org/10.1016/j.neuron.2019.10.017>

Jin, P., L.Y. Jan, and Y.N. Jan. 2020. Mechanosensitive ion channels: Structural features relevant to mechanotransduction mechanisms. *Annu. Rev. Neurosci.* 43:207–229. <https://doi.org/10.1146/annurev-neuro-070918-050509>

Jojoa-Cruz, S., B. Burendei, W.H. Lee, and A.B. Ward. 2024a. Structure of mechanically activated ion channel OSCA2.3 reveals mobile elements in the transmembrane domain. *Structure.* 32:157–167.e5. <https://doi.org/10.1016/j.str.2023.11.009>

Jojoa-Cruz, S., A.E. Dubin, W.H. Lee, and A.B. Ward. 2024b. Structure-guided mutagenesis of OSCAs reveals differential activation to mechanical stimuli. *Elife.* 12:RP93147. <https://doi.org/10.7554/elife.93147>

Jojoa-Cruz, S., K. Saotome, S.E. Murthy, C.C.A. Tsui, M.S. Sansom, A. Patapoutian, and A.B. Ward. 2018. Cryo-EM structure of the mechanically activated ion channel OSCA1.2. *Elife.* 7:e41845. <https://doi.org/10.7554/elife.41845>

Kawashima, Y., G.S.G. Gélyéoc, K. Kurima, V. Labay, A. Lelli, Y. Asai, T. Makishima, D.K. Wu, C.C. Della Santina, J.R. Holt, and A.J. Griffith. 2011. Mechanotransduction in mouse inner ear hair cells requires transmembrane channel-like genes. *J. Clin. Invest.* 121:4796–4809. <https://doi.org/10.1172/JCI60405>

Kefauver, J.M., A.B. Ward, and A. Patapoutian. 2020. Discoveries in structure and physiology of mechanically activated ion channels. *Nature.* 587: 567–576. <https://doi.org/10.1038/s41586-020-2933-1>

Kloda, A., and B. Martinac. 2002. Common evolutionary origins of mechanosensitive ion channels in Archaea, Bacteria and cell-walled Eukarya. *Archaea.* 1:35–44. <https://doi.org/10.1155/2002/419261>

Kortmann, J., K. Huang, M.-C. Tsai, K. Barck, A. Jacobson, C.D. Austin, D. Dunlap, C. Chaloumi, S. Jeet, A. Balestrini, et al. 2023. Lung-innervating neurons expressing Tmc3 can induce broncho-constriction and dilation with direct consequences for the respiratory cycle. *bioRxiv.* <https://doi.org/10.1101/2023.08.24.554567> (Preprint posted August 26, 2023).

Kurima, K., L.M. Peters, Y. Yang, S. Riazuddin, Z.M. Ahmed, S. Naz, D. Arnaud, S. Drury, J. Mo, T. Makishima, et al. 2002. Dominant and recessive deafness caused by mutations of a novel gene, TMC1, required for cochlear hair-cell function. *Nat. Genet.* 30:277–284. <https://doi.org/10.1038/ng842>

Kurima, K., Y. Yang, K. Sorber, and A.J. Griffith. 2003. Characterization of the transmembrane channel-like (TMC) gene family: Functional clues from hearing loss and epidermolyticus verruciformis. *Genomics.* 82: 300–308. [https://doi.org/10.1016/s0888-7543\(03\)00154-x](https://doi.org/10.1016/s0888-7543(03)00154-x)

Le, S.C., P. Liang, A.J. Lowry, and H. Yang. 2021. Gating and regulatory mechanisms of TMEM16 ion channels and scramblases. *Front. Physiol.* 12:787773. <https://doi.org/10.3389/fphys.2021.787773>

Le, T., Z. Jia, S.C. Le, Y. Zhang, J. Chen, and H. Yang. 2019. An inner activation gate controls TMEM16F phospholipid scrambling. *Nat. Commun.* 10: 1846. <https://doi.org/10.1038/s41467-019-09778-7>

Li, B., S. Li, H. Zheng, and Z. Yan. 2021. Nanchung and inactive define pore properties of the native auditory transduction channel in *Drosophila*. *Proc. Natl. Acad. Sci. USA.* 118:e2106459118. <https://doi.org/10.1073/pnas.2106459118>

Li, K., Y. Guo, Y. Wang, R. Zhu, W. Chen, T. Cheng, X. Zhang, Y. Jia, T. Liu, W. Zhang, et al. 2024. *Drosophila* TMEM63 and mouse TMEM63A are lysosomal mechanosensory ion channels. *Nat. Cell Biol.* 26:393–403. <https://doi.org/10.1038/s41556-024-01353-7>

Li, S., B. Li, L. Gao, J. Wang, and Z. Yan. 2022. Humidity response in *Drosophila* olfactory sensory neurons requires the mechanosensitive channel TMEM63. *Nat. Commun.* 13:3814. <https://doi.org/10.1038/s41467-022-31253-z>

Liu, H., C.M. Tse, and S. Dang. 2025. Capturing the native structure of membrane proteins using vesicles. *Proc. Natl. Acad. Sci. USA.* 122: e2423407122. <https://doi.org/10.1073/pnas.2423407122>

Liu, X., J. Wang, and L. Sun. 2018. Structure of the hyperosmolality-gated calcium-permeable channel OSCA1.2. *Nat. Commun.* 9:5060. <https://doi.org/10.1038/s41467-018-07564-5>

Lowry, A.J., P. Liang, M. Song, Y. Wan, Z.M. Pei, H. Yang, and Y. Zhang. 2024. TMEM16 and OSCA/TMEM63 proteins share a conserved potential to permeate ions and phospholipids. *Elife.* 13:RP96957. <https://doi.org/10.7554/elife.96957>

Maity, K., J.M. Heumann, A.P. McGrath, N.J. Kopcho, P.-K. Hsu, C.-W. Lee, J.H. Mapes, D. Garza, S. Krishnan, G.P. Morgan, et al. 2019. Cryo-EM structure of OSCA1.2 from *Oryza sativa* elucidates the mechanical basis of potential membrane hyperosmolality gating. *Proc. Natl. Acad. Sci. USA.* 116:14309–14318. <https://doi.org/10.1073/pnas.1900774116>

Marshall, K.L., D. Saade, N. Ghitani, A.M. Coombs, M. Szczot, J. Keller, T. Ogata, I. Daou, L.T. Stowers, C.G. Bönnemann, et al. 2020. PIEZO2 in sensory neurons and urothelial cells coordinates urination. *Nature.* 588: 290–295. <https://doi.org/10.1038/s41586-020-2830-7>

Medrano-Soto, A., G. Moreno-Hagelsieb, D. McLaughlin, Z.S. Ye, K.J. Hengargo, and M.H. Saier Jr. 2018. Bioinformatic characterization of the Anoctamin Superfamily of Ca^{2+} -activated ion channels and lipid scramblases. *PLoS One.* 13:e0192851. <https://doi.org/10.1371/journal.pone.0192851>

Minegishi, T., H. Hasebe, T. Aoyama, K. Naruse, Y. Takahashi, and N. Inagaki. 2025. Mechanical signaling through membrane tension induces somal translocation during neuronal migration. *EMBO J.* 44:767–780. <https://doi.org/10.1038/s44318-024-00326-8>

Miyata, Y., K. Takahashi, Y. Lee, C.S. Sultan, R. Kurabayashi, M. Takahashi, K. Hata, T. Bamba, Y. Izumi, K. Liu, et al. 2025. Membrane structure-responsive lipid scrambling by TMEM63B to control plasma membrane lipid distribution. *Nat. Struct. Mol. Biol.* 32:185–198. <https://doi.org/10.1038/s41594-024-01411-6>

Mun, M., and J.R. Holt. 2025. A contemporary view of mechanosensory transduction in auditory hair cells. *Biophys. J.* S0006-3495(25)00375-3. <https://doi.org/10.1016/j.bpj.2025.06.015>

Murthy, S.E., A.E. Dubin, T. Whitwam, S. Jojoa-Cruz, S.M. Cahalan, S.A.R. Mousavi, A.B. Ward, and A. Patapoutian. 2018. OSCA/TMEM63 are an evolutionarily conserved family of mechanically activated ion channels. *Elife*. 7:e41844. <https://doi.org/10.7554/eLife.41844>

Niu, H., M. Maruoka, Y. Noguchi, H. Kosako, and J. Suzuki. 2024. Phospholipid scrambling induced by an ion channel/metabolite transporter complex. *Nat. Commun.* 15:7566. <https://doi.org/10.1038/s41467-024-51939-w>

Nonomura, K., S.-H. Woo, R.B. Chang, A. Gillich, Z. Qiu, A.G. Francisco, S.S. Ranade, S.D. Liberles, and A. Patapoutian. 2017. Piezo2 senses airway stretch and mediates lung inflation-induced apnoea. *Nature*. 541: 176–181. <https://doi.org/10.1038/nature20793>

Orphal, M., A. Gillespie, K. Böhme, J. Subrova, A. Eisenreich, and R. Kreutz. 2020. TMEM63C, a potential novel target for albuminuria development, is regulated by microRNA-564 and transforming growth factor beta in human renal cells. *Kidney Blood Press. Res.* 45:850–862. <https://doi.org/10.1159/000508477>

Pan, B., N. Akyuz, X.P. Liu, Y. Asai, C. Nist-Lund, K. Kurima, B.H. Derfler, B. György, W. Limapichat, S. Walujkar, et al. 2018. TMCI forms the pore of mechanosensory transduction channels in vertebrate inner ear hair cells. *Neuron*. 99:736–753.e6. <https://doi.org/10.1016/j.neuron.2018.07.033>

Pan, B., G.S. Gélécoc, Y. Asai, G.C. Horwitz, K. Kurima, K. Ishikawa, Y. Kawashima, A.J. Griffith, and J.R. Holt. 2013. TMCI and TMC2 are components of the mechanotransduction channel in hair cells of the mammalian inner ear. *Neuron*. 79:504–515. <https://doi.org/10.1016/j.neuron.2013.06.019>

Pei, S., Q. Tao, W. Li, G. Qi, B. Wang, Y. Wang, S. Dai, Q. Shen, X. Wang, X. Wu, et al. 2024. Osmosensor-mediated control of Ca^{2+} spiking in pollen germination. *Nature*. 629:1118–1125. <https://doi.org/10.1038/s41586-024-07445-6>

Peters, C.J., J.M. Gilchrist, J. Tien, N.P. Bethel, L. Qi, T. Chen, L. Wang, Y.N. Jan, M. Grabe, and L.Y. Jan. 2018. The sixth transmembrane segment is a major gating component of the TMEM16A calcium-activated chloride channel. *Neuron*. 97:1063–1077.e4. <https://doi.org/10.1016/j.neuron.2018.01.048>

Pu, S., Y. Wu, F. Tong, W.-J. Du, S. Liu, H. Yang, C. Zhang, B. Zhou, Z. Chen, X. Zhou, et al. 2023. Mechanosensitive ion channel TMEM63A gangs up with local macrophages to modulate chronic post-amputation pain. *Neurosci. Bull.* 39:177–193. <https://doi.org/10.1007/s12264-022-00910-0>

Qin, Y., D. Yu, D. Wu, J. Dong, W.T. Li, C. Ye, K.C. Cheung, Y. Zhang, Y. Xu, Y. Wang, et al. 2023. Cryo-EM structure of TMEM63C suggests it functions as a monomer. *Nat. Commun.* 14:7265. <https://doi.org/10.1038/s41467-023-42956-2>

Ranade, S.S., S.-H. Woo, A.E. Dubin, R.A. Moshourab, C. Wetzel, M. Petrus, J. Mathur, V. Bégay, B. Coste, J. Mainquist, et al. 2014. Piezo2 is the major transducer of mechanical forces for touch sensation in mice. *Nature*. 516:121–125. <https://doi.org/10.1038/nature13980>

Schroeder, B.C., T. Cheng, Y.N. Jan, and L.Y. Jan. 2008. Expression cloning of TMEM16A as a calcium-activated chloride channel subunit. *Cell*. 134: 1019–1029. <https://doi.org/10.1016/j.cell.2008.09.003>

Schulz, A., N.V. Müller, N.A. van de Lest, A. Eisenreich, M. Schmidbauer, A. Barysenka, B. Purfürst, A. Spörbert, T. Lorenzen, A.M. Meyer, et al. 2019. Analysis of the genomic architecture of a complex trait locus in hypertensive rat models links Tmem63c to kidney damage. *Elife*. 8: e42068. <https://doi.org/10.7554/eLife.42068>

Shan, Y., M. Zhang, M. Chen, X. Guo, Y. Li, M. Zhang, and D. Pei. 2024. Activation mechanisms of dimeric mechanosensitive OSCA/TMEM63 channels. *Nat. Commun.* 15:7504. <https://doi.org/10.1038/s41467-024-51800-0>

Sukharev, S.I., B. Martinac, V.Y. Arshavsky, and C. Kung. 1993. Two types of mechanosensitive channels in the *Escherichia coli* cell envelope: Solubilization and functional reconstitution. *Biophys. J.* 65:177–183. [https://doi.org/10.1016/S0006-3495\(93\)81044-0](https://doi.org/10.1016/S0006-3495(93)81044-0)

Sun, W., S. Chi, Y. Li, S. Ling, Y. Tan, Y. Xu, F. Jiang, J. Li, C. Liu, G. Zhong, et al. 2019. The mechanosensitive Piezol1 channel is required for bone formation. *Elife*. 8:e47454. <https://doi.org/10.7554/eLife.47454>

Tábara, L.C., F. Al-Salmi, R. Maroofian, A.M. Al-Futaisi, F. Al-Murshedi, J. Kennedy, J.O. Day, T. Courtin, A. Al-Khayat, H. Galedari, et al. 2022. TMEM63C mutations cause mitochondrial morphology defects and underlie hereditary spastic paraparesis. *Brain*. 145:3095–3107. <https://doi.org/10.1093/brain/awac123>

Tao, X., C. Zhao, and R. MacKinnon. 2023. Membrane protein isolation and structure determination in cell-derived membrane vesicles. *Proc. Natl. Acad. Sci. USA*. 120:e2302325120. <https://doi.org/10.1073/pnas.2302325120>

Thor, K., S. Jiang, E. Michard, J. George, S. Scherzer, S. Huang, J. Dindas, P. Derbyshire, N. Leitão, T.A. DeFalco, et al. 2020. The calcium-permeable channel OSCA1.3 regulates plant stomatal immunity. *Nature*. 585: 569–573. <https://doi.org/10.1038/s41586-020-2702-1>

Tonduti, D., E. Mura, S. Masnada, E. Bertini, C. Aiello, D. Zini, L. Parmeggiani, G. Cantalupo, G. Talenti, P. Veggiani, et al. 2021. Spinal cord involvement and paroxysmal events in “Infantile Onset Transient Hypomyelination” due to TMEM63A mutation. *J. Hum. Genet.* 66:1035–1037. <https://doi.org/10.1038/s10038-021-00921-1>

Tu, J.-J., C. Ye, X.-Y. Teng, Y.-Z. Zang, X.-Y. Sun, S. Chen, J. Chen, and Y.S. Shi. 2025. Osmosensor TMEM63B facilitates insulin secretion in pancreatic β -cells. *Sci. China Life Sci.* 68:1714–1726. <https://doi.org/10.1007/s11427-024-2833-3>

Tu, J.-J., Y.-Y. Zang, Y.S. Shi, and X.-Y. Teng. 2024. The TMEM63B channel facilitates intestinal motility and enhances proliferation of intestinal stem cells. *Cells*. 13:1784. <https://doi.org/10.3390/cells13211784>

Vetro, A., C. Pelorosso, S. Balestrini, A. Masi, S. Hambleton, E. Argilli, V. Conti, S. Giubbolini, R. Barrick, G. Bergant, et al. 2023. Stretch-activated ion channel TMEM63B associates with developmental and epileptic encephalopathies and progressive neurodegeneration. *Am. J. Hum. Genet.* 110:1356–1376. <https://doi.org/10.1016/j.ajhg.2023.06.008>

Vreugde, S., A. Erven, C.J. Kros, W. Marcotti, H. Fuchs, K. Kurima, E.R. Wilcox, T.B. Friedman, A.J. Griffith, R. Balling, et al. 2002. Beethoven, a mouse model for dominant, progressive hearing loss DFNA36. *Nat. Genet.* 30:257–258. <https://doi.org/10.1038/ng848>

Walujkar, S., J.M. Lotthammer, C.R. Nisler, J.C. Sudar, A. Ballesteros, and M. Sotomayor. 2021. In silico electrophysiology of inner-ear mechanotransduction channel TMCI models. *bioRxiv*. <https://doi.org/10.1101/2021.09.17.460860> (Preprint posted September 18, 2021).

Wang, J., Y. Yin, L. Yang, J. Qin, Z. Wang, C. Qiu, Y. Gao, G. Lu, F. Gao, Z.J. Chen, et al. 2024. TMCI deficiency causes acrosome biogenesis defects and male infertility in mice. *Elife*. 13:RP95888. <https://doi.org/10.7554/eLife.95888>

Wang, Y., Y. Guo, G. Li, C. Liu, L. Wang, A. Zhang, Z. Yan, and C. Song. 2021. The push-to-open mechanism of the tethered mechanosensitive ion channel NompC. *Elife*. 10:e58388. <https://doi.org/10.7554/eLife.58388>

Woo, S.-H., S. Ranade, A.D. Weyer, A.E. Dubin, Y. Baba, Z. Qiu, M. Petrus, T. Miyamoto, K. Reddy, E.A. Lumpkin, et al. 2014. Piezo2 is required for Merkel-cell mechanotransduction. *Nature*. 509:622–626. <https://doi.org/10.1038/nature13251>

Wu, D., L. Xu, W.-M. Cai, S.-Y. Zhan, G. Wan, Y. Xu, and Y.S. Shi. 2023. A splicing-dependent ER retention signal regulates surface expression of the mechanosensitive TMEM63B cation channel. *J. Biol. Chem.* 299: 102781. <https://doi.org/10.1016/j.jbc.2022.102781>

Wu, D., Y.Y. Zang, Y.Y. Shi, C. Ye, W.-M. Cai, X.-H. Tang, L. Zhao, Y. Liu, Z. Gan, G.-Q. Chen, et al. 2020. Distant coupling between RNA editing and alternative splicing of the osmosensitive cation channel Tmem63b. *J. Biol. Chem.* 295:18199–18212. <https://doi.org/10.1074/jbc.RA120.016049>

Wu, W., S. Liu, L. Tian, C. Li, Y. Jiang, J. Wang, Y. Lv, J. Guo, D. Xing, Y. Zhai, et al. 2022. Identification of microtubule-associated biomarkers in diffuse large B-cell lymphoma and prognosis prediction. *Front. Genet.* 13: 1092678. <https://doi.org/10.3389/fgene.2022.1092678>

Wu, X., T. Shang, X. Lü, D. Luo, and D. Yang. 2024. A monomeric structure of human TMEM63A protein. *Proteins*. 92:750–756. <https://doi.org/10.1002/prot.26660>

Wu, Z., N. Grillet, B. Zhao, C. Cunningham, S. Harkins-Perry, B. Coste, S. Ranade, N. Zebarjadi, M. Beurg, R. Fettiplace, et al. 2017. Mechanosensory hair cells express two molecularly distinct mechanotransduction channels. *Nat. Neurosci.* 20:24–33. <https://doi.org/10.1038/nn.4449>

Yan, H., G. Helman, S.E. Murthy, H. Ji, J. Crawford, T. Kubisiak, S.J. Bent, J. Xiao, R.J. Taft, A. Coombs, et al. 2019. Heterozygous variants in the mechanosensitive ion channel TMEM63A result in transient hypomyelination during infancy. *Am. J. Hum. Genet.* 105:996–1004. <https://doi.org/10.1016/j.ajhg.2019.09.011>

Yan, Z., W. Zhang, Y. He, D. Gorczyca, Y. Xiang, L.E. Cheng, S. Meltzer, L.Y. Jan, and Y.N. Jan. 2013. Drosophila NompC is a mechanotransduction channel subunit for gentle-touch sensation. *Nature*. 493:221–225. <https://doi.org/10.1038/nature11685>

Yang, G., M. Jia, G. Li, Y.-Y. Zang, Y.-Y. Chen, Y.-Y. Wang, S.-Y. Zhan, S.-X. Peng, G. Wan, W. Li, et al. 2024. TMEM63B channel is the osmosensor required for thirst drive of interoceptive neurons. *Cell Discov.* 10:1. <https://doi.org/10.1038/s41421-023-00628-x>

Yang, Y.D., H. Cho, J.Y. Koo, M.H. Tak, Y. Cho, W.S. Shim, S.P. Park, J. Lee, B. Lee, B.M. Kim, et al. 2008. TMEM16A confers receptor-activated

calcium-dependent chloride conductance. *Nature*. 455:1210–1215. <https://doi.org/10.1038/nature07313>

Ye, C., T.-Z. Zhang, Y.-Y. Zang, Y.S. Shi, and G. Wan. 2024. TMEM63B regulates postnatal development of cochlear sensory epithelia via thyroid hormone signaling. *J. Genet. Genomics*. 51:673–676. <https://doi.org/10.1016/j.jgg.2023.12.006>

Yuan, F., H. Yang, Y. Xue, D. Kong, R. Ye, C. Li, J. Zhang, L. Theprungsirikul, T. Shrift, B. Kricheldorf, et al. 2014. OSCA1 mediates osmotic-stress-evoked Ca^{2+} increases vital for osmosensing in *Arabidopsis*. *Nature*. 514: 367–371. <https://doi.org/10.1038/nature13593>

Zhang, M., Y. Shan, C.D. Cox, and D. Pei. 2023a. A mechanical-coupling mechanism in OSCA/TMEM63 channel mechanosensitivity. *Nat. Commun.* 14:3943. <https://doi.org/10.1038/s41467-023-39688-8>

Zhang, M., D. Wang, Y. Kang, J.-X. Wu, F. Yao, C. Pan, Z. Yan, C. Song, and L. Chen. 2018. Structure of the mechanosensitive OSCA channels. *Nat. Struct. Mol. Biol.* 25:850–858. <https://doi.org/10.1038/s41594-018-0117-6>

Zhang, T.-M., L. Liao, S.-Y. Yang, M.-Y. Huang, Y.-L. Zhang, L. Deng, S.-Y. Hu, F. Yang, F.-L. Zhang, Z.-M. Shao, and D.-Q. Li. 2023b. TOLLIP-mediated autophasic degradation pathway links the VCP-TMEM63A-DERL1 signaling axis to triple-negative breast cancer progression. *Autophagy*. 19: 805–821. <https://doi.org/10.1080/15548627.2022.2103992>

Zhang, W., L.E. Cheng, M. Kittelmann, J. Li, M. Petkovic, T. Cheng, P. Jin, Z. Guo, M.C. Göpfert, L.Y. Jan, and Y.N. Jan. 2015. Ankyrin repeats convey force to gate the NOMPC mechanotransduction channel. *Cell*. 162: 1391–1403. <https://doi.org/10.1016/j.cell.2015.08.024>

Zheng, W., and J.R. Holt. 2021. The mechanosensory transduction machinery in inner ear hair cells. *Annu. Rev. Biophys.* 50:31–51. <https://doi.org/10.1146/annurev-biophys-062420-081842>

Zheng, W., A.J. Lowry, H.E. Smith, J. Xie, S. Rawson, C. Wang, J. Ou, M. Sotomayor, T.M. Fu, H. Yang, and J.R. Holt. 2025. Structural and functional basis of mechanosensitive TMEM63 channelopathies. *Neuron*. 113:2474–2489.e5. <https://doi.org/10.1016/j.neuron.2025.05.009>

Zheng, W., S. Rawson, Z. Shen, E. Tamiselvan, H.E. Smith, J. Halford, C. Shen, S.E. Murthy, M.H. Ulbrich, M. Sotomayor, et al. 2023. TMEM63 proteins function as monomeric high-threshold mechanosensitive ion channels. *Neuron*. 111:3195–3210.e7. <https://doi.org/10.1016/j.neuron.2023.07.006>

Zou, W., S. Deng, X. Chen, J. Ruan, H. Wang, W. Zhan, J. Wang, Z. Liu, and Z. Yan. 2025. TMEM63B functions as a mammalian hyperosmolar sensor for thirst. *Neuron*. 113:1430–1445.e5. <https://doi.org/10.1016/j.neuron.2025.02.012>